International Journal of Semiconductor
Science & Technology (IJSST)
ISSN 2250-1576
Vol. 3, Issue 4, Oct 2013, 11-18

PERFORMANCE OF A NANOSTRUCTURED PbS/Si HETROJUNCTION DETECTOR DEPOSITED BY CBD

ALI M. MOUS, SELMA M. H. AL-JAWAD & SUAD M. KADHIM AL-SHAMMARI

Department of Applied Science, University of Technology, Baghdad, Iraq

ABSTRACT

The present work demonstrates the electrical transport and photo response properties of nano PbS / n-Si hetero junction grown by chemical bath deposition. Polycrystalline nature of nanostructured PbS is confirmed by the X-ray diffraction. XRD measurements show that these nano films have sharp peaks at $2\theta=30^{o}$ indicating a preferred orientation along (200) plane, with grain size increase with deposition time. The electrical transport properties of the device were studied at room temperature. The diode shows good ideality factor and rectifying behavior with an on/off ratio change with deposition time. Experimental data showed that the responsivity cutoff point corresponds to the absorption edge of the siliconsubstrate, and films photosensitivity depends on the film thickness

KEYWORDS: Nano PbS, Hetrojunction, Chemical Bath Deposition

INTRODUCTION

Nano-structured layers in thin film photovoltaic devices offer three important advantages allowing more design flexibility in the absorber and window layers (1, 2). Lead sulfide (PbS) has a relatively small band gap (0.41 eV at 300 K) The band gap of PbS can be easily adjusted up to a few electron volts when in the form of nanometer sized dots (3) . A great deal of research efforts has been devoted to the synthesis of PbS nanoparticles of varying size in a controlled manner. Vacuum evaporation [4], hot-wall epitaxy and molecular-beam epitaxy [4, 5] are among the most successful "dry" methods for PbS synthesis. The frequently used "wet" methods include spray pyrolysis [6], chemical bath deposition [7] and electrochemical deposition [8]. Earlier investigations into the fundamental performance of nano PbS hetrojunction deposited on different substrates confirm their ability to become a versatile technological platform for the creation of better optoelectronic devices [8–12].Herein, we described electronic modulation of the fundamental characteristics (quantum efficiency, spectral responsivity) of a nanoPbS /n-Si hetrojunction junction fabricated in the Al/PbS/Si/In architecture, where the nanoparticle films are chemically deposited from solutions.

EXPERIMENT

Nanostructures PbS thin films were prepared on clean silicon and glass substrates using the Chemical Bath Deposition (CBD) method. The basic principle of the CBD method is in the controlled generation of the metal and chalcogenides ions in an alkaline medium and their precipitation on the substrate in order to form a film. Silicon wafers used for fabricating PbS/Si heterojunction were mirror like p-type (111) orientation with resistivity of (1.5–4 Ω•cm) and (500 µm) thickness. They were rinsed in acetone and ethanol in order to remove dirt and oil, while native oxide layer was removed by etching in dilute (1:10) HF: H2O solution.

The starting materials in the preparation of lead sulfate (PbS) includes lead acetate [Pb (CH3COO)2.2H2O], Potassium hydroxide (KOH), thiourea [(NH2)2.CS], triethanolamine TEAand distilled water. The lead acetate is the source of cation (Pb2+) and thiourea is the source of anion (S2─). KOH is used to provide an alkaline medium (10 -12.5 pH).

The nano PbS/n-Si hetrojunction was deposited from a solution having optimal deposition parameters which gives higher efficiency including deposition time 15 min , pH 11.5 ,T =30ºC , M_{Pb} 0.25M , M_{Sc} 0.5 M. Electrodes were deposited on both sides of the PbS/p-Si. Ohmic contacts from high purity aluminum wire 5N with 200nm thickness onto the back surface of Si, and indium on PbS layer were performed through a metal mask.

Dark current–voltage measurements were carried out by applying a voltage to the sample from a stabilized d.c. power supply, type L 30–2 Farnell of range (0.1–5)V. The current passing through the device was measured using a Keithley (602) electrometer. From I –V characteristics, the ideality factor was calculated using the following equation

$$\beta = (q/KT)(dv / d \ln I) \quad (1)$$

while the rectification ratio RF is calculated according to the following Eq. (10)

$$RF = \frac{I_f}{I_r} \text{ For } V \geq \frac{3KT}{q} \quad (2)$$

Capacitance–Voltage characteristics of the heterojunction were measured using a PM 6306 Programmable LRC meter supplied by Fluke the measurement is carried out at ferquncy of 200 kHz . The reverse bias voltage ranged from (0.5–5) V. the built – in potential V_{bi} were determined from intercept at $1/C^2 =0$ by extrapolating the curve to the voltage axis.

The spectral responsivity of the PbS/Si heterojunction was measured using a monochromator with spectral range of (360–1000) nm. Power calibration was established using a standard silicon power meter. This measurement was performed with a reverse bias (1V). The Responsivity R_λ and quantum efficiency were calculated from the following equations (11)

$$R_\lambda = \frac{I_{ph}}{P_{in}}, \eta = \frac{I_{ph}/q}{P_{in}/h\upsilon} \quad (3)$$

RESULTS AND DISCUSSIONS

Structural Analysis

The structural characteristics of the as-grown nanostructure PbS were evaluated by XRD. Figure (1) shows predominant orientation peak at $2\theta=30^o$ indicating a preferred orientation along (200) plane of reflection corresponding to the cubic (galena) phase. Compared to the reference data from PbS single crystal as shown in Table (1), the peaks in the XRD diffraction shift into the region of higher θ (smaller lattice parameters), indicating stress in the grains. The a-lattice constant of Si is 0.5261 nm, while alattice constant calculated for PbS is 0.5936 nm. The lattice mismatch hence is 11.

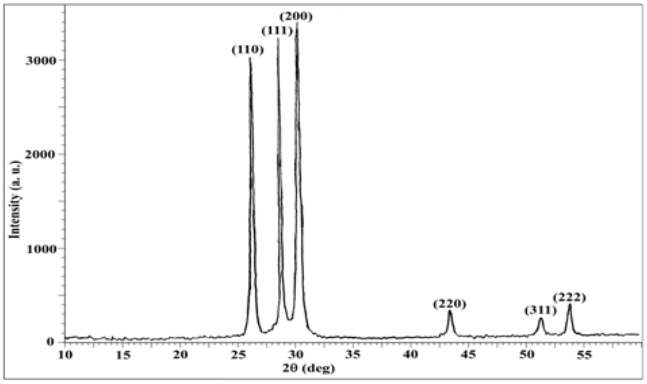

Figure 1: X – Ray Diffraction of Nano PbS/n-Si

Table 1: Shows the Structural Analysis of Deposited Film as a Function of Deposition Time

Deposition Time (min)	(2θ) Degree	hkl	d(nm) XRD	d(nm) ASTM	a(nm) XRD	δ%	G.S (nm)
15	30	(200)	0.2966	0.2963	0.5964	0.0612	4.9
30	29.9	(200)	0.2978	0.2963	0.5938	0.0432	6.4
45	30.9	(200)	0.2981	0.2963	0.5921	0.0152	9.2
60	30	(200)	0.2973	0.2963	0.5864	0.0088	11.3

Current–Voltage Characteristics

The dark I-V characteristics at forward and reverse bias for different deposition times of the nano PbS/n-Si heterojunction measured at room temperature are shown in Figure (2). The PbS films were unintentionally doped show an p-type conductivity, Table (2) shows carrier's concentration, mobility and band gap values at different deposition time.

The diode gives good ideality factor and exhibits good rectifying behavior with an on/off ratio change with deposition time as shown in Table (3). To understand the rectifying behavior observed in these hetrojunctions, one first notes that there exists an offset between the conduction bands of PbS and Si. Forward dark current generated due to the flow of majority carriers where the applied voltage injects majority carriers lead to the decreasing of the built-in potential, as well as the width of the depletion layer. As the majority and minority carrier concentrations are higher than the intrinsic carrier concentration (n^2_i<np), so the crystal to restore the equilibrium situation the excess of charge carriers will under goes the recombination current at the low voltage region (0-0.25) Volt.

This is because the excitation of electrons from valence band (V.B.) to conduction band (C.B.) will recombine them with the holes which are found at the V.B., and this is observed by the little increase in recombination current at low voltage region [80]. On the other hand, the tunneling current is represented at the high voltage region (>0.25), where there is a fast exponential increase in the current magnitude with increasing the voltage and this is called diffusion current, which dominates the process.

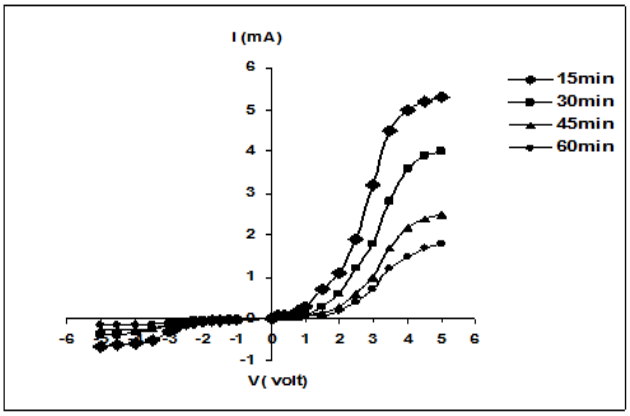

Figure 2: I – V Characteristic for Nano PbS/n-Si Prepared at Different Deposition Times (T=30°C, pH=11.6, MPb=0.25M, MSc=0.5M)

Table 2: Shows Carrier's Concentration, and Band Gap Values at Different Deposition Time

Deposition Time(min)	Carriers Cons.* 10^{15} $(cm)^{-3}$	Mobility (cm^2/V.S)	Band Gap (eV)
15	6.23	3.7	2.32
30	8.15	2.7	2.29
45	9.89	1.23	2.15
60	12.8	0.86	1.96

Table 3: Shows Saturation Current, Ideal Factor and Rectifying Ratio at Different Deposition Time

Deposition Conditions	Is(μA)	β factor	R.F at 5V
15 min	0.42	1.41	30
30 min	0.4	1.36	26.8
45 min	0.23	1.25	22.8
60 min	0.145	1.21	23.3

In the case of reverse bias current also contains two regions. In the first region of low voltage (<0.25) volt, the current slightly increases with increasing of the applied voltage, and the generation current dominates, while at the second high voltage region (>0.25) volt, the diffusion current dominates. Also we can observe from figure (2) that the value of the current decreases with increasing of deposition time of films which is attributed to evolving defects and dislocations that have an effect on the mobility of charge carriers. Also these defects evolutions allow energy levels to be within the energy gap; these defects are within the depletion region act as active recombination centers, and consequently they decrease the current flow across the junction

Capacitance – Voltage Measurement

The junction capacitance variations as a function of the reverse bias (0 –5) volt at frequency equal to 200 KHz has been studied for different deposition times. It is clear that the capacitance decreases in a non-linear with increasing of the reverse bias voltages shown in figure (3). such behavior is attributed to the increasing of the depletion region width which is related to junction capacitance [12]. The increasing in the depletion region width leads to decreasing in the value of built-in potential. The plots of the inverse capacitance square against applied reverse bias voltage revealed straight line relationship which means that the junction was of an abrupt type. The interception of the straight line with the voltage axis at ($1/C^2 = 0$) points, represents the built-in potential, results of V_{bi} as a function of deposition time are given in Table (4).

Table 4: Values of Built- in Potential for Different Deposition Time

Deposition Time (min)	Built-in Potential(eV)
15	0.6
30	0.5
45	0.45
60	0.4

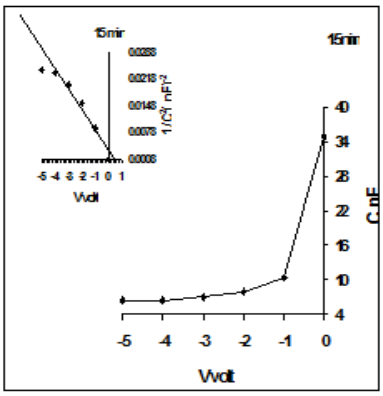

Figure 3: Junction C – V Characteristics, Inset is $1/c^2$Vs Bias Voltage

Illuminated Current – Voltage Measurements Characteristics

Figure (4) shows the I – V characteristic of nano PbS/n-Si under various levels of illumination. The photocurrent increases with increasing the bias voltage, such results could be related to the increasing of depletion layer width, and

hence increasing in the concentration of absorbed photons in a region where internal electric field extended [13].The increase of the incident light intensity causes increase in photocurrent due to the increase in number of photo generated charge carriers that float within the depletion region and diffusion carriers region, which in turns reducing the grain boundaries and improvement of structure causes the increase of the mobility. Also we can see from figure (4) that the photocurrent decreases with increasing the deposition time. This is due to increase the structural defect leading to decrease of the mobility; hence, photocarriers generated far from the junction will not diffuse and will not contribute to the final photocurrent..

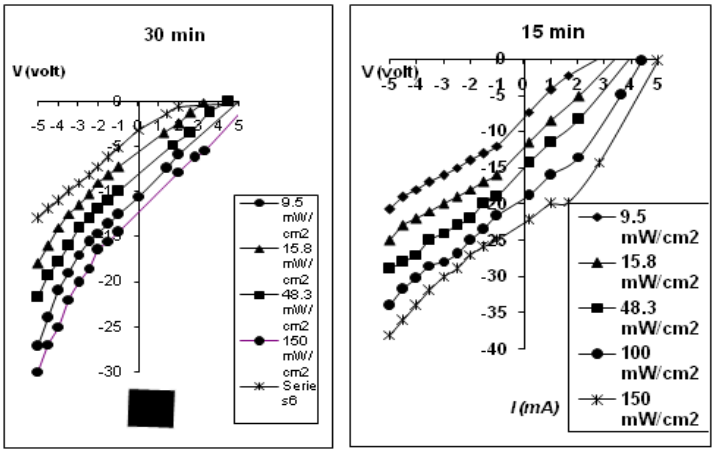

Figure 4: I – V Characteristic for Nano PbS/n-Si under Various Levels of Illumination at 15 and 30 min. Deposition Time(T=30°C, pH=11.6, MPb=0.25M, MSc=0.5M)

Spectral Responsivity of Nano PbS/n-Si Detectors

The spectral responsivity specifies the performance range of a detector. Figure (5) shows the variation in spectral responsivity for nano- PbS/n-Si prepared at different deposition times. the spectral responsivity comprised of three distinct regions. The first region at short wavelength where responsivity increases with increasing wavelength and this increase relates to the high absorption coefficient. The second region shows an increase responsivity passing through the maximum value between (650 -750) nm corresponding to light absorption at transition region on silicon side. The third region shows that responsivity decreases with an increase in wavelength. The cutoff point corresponds to the absorption edge of the siliconsubstrate. The smaller responsivity at longer wavelength is attributed to the carriers generated deep in the silicon substrate, where the spectrum extends to the IR region. The higher responsivity with 15 min. is probably due to the greater value of carriers mobility (3.7cm^2/V.S) and higher built in potential (0.6eV)..

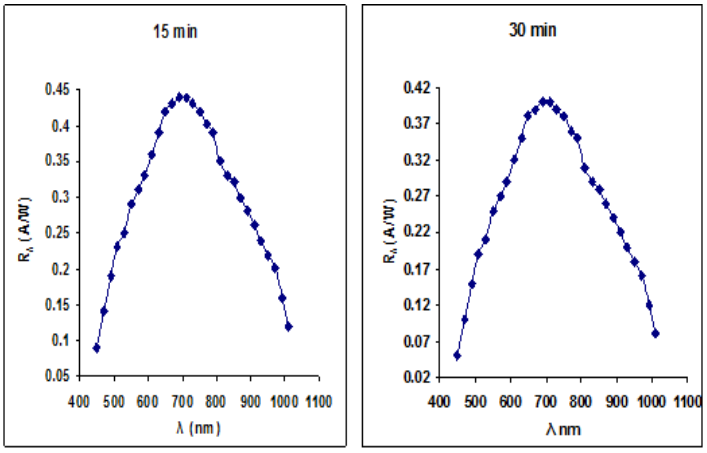

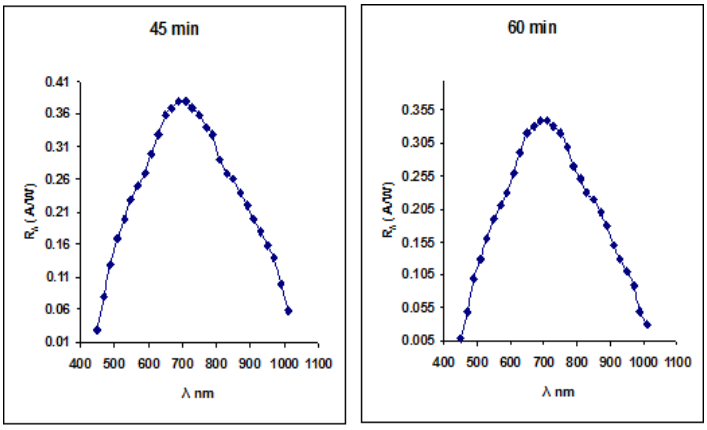

Figure 5: Spectral Responsivity at Different Deposition Time (T=30°C, pH=11.6, MPb=0.25M, MSc=0.5M)

Quantum Efficiency

Figure (6) show the variation of quantum efficiency with wavelength for nano-PbS/n-Si prepared at different times. All the explanations mentioned on responsivity can be drawn to the quantum efficiency because quantum efficiency is a function of spectral responsivity [14].The effect of deposition time on the maximum quantum efficiency is very obvious in figure (7). The quantum efficiency decreases with increasing deposition time, and this can be attributed to

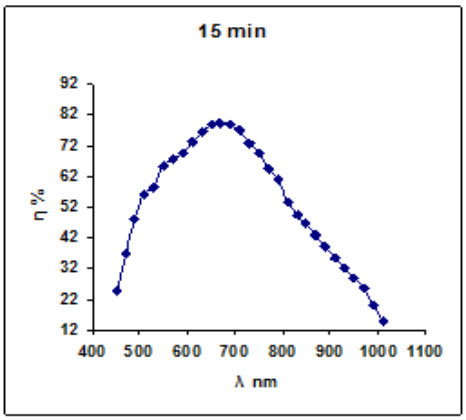

Figure 6: Quantum Efficiency of Nano PbS/n-Si

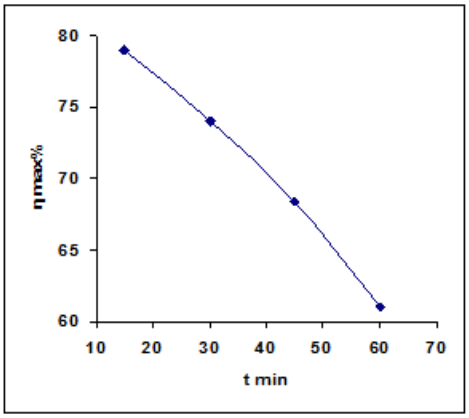

Figure 7: Quantum Efficiency of Nano PbS /n-Si as a Prepared at 15 Deposition Time Function of Deposition Time

CONCLUSIONS

We have shown the possibility of preparing nano PbS/n-Si using chemical bath deposition. The diode gives good ideality factor and exhibits good rectifying behavior with an on/off ratio change with deposition time. The photocurrent

increases with increasing the bias voltage. the photocurrent decreases with increasing the deposition time. This is due to increase the structural defect leading to decrease of the mobility. Spectral responsivity passing through the maximum value between (650 -750) nm corresponding to light absorption at transition region on silicon side. The quantum efficiency decreases with increasing deposition time.

REFERENCES

1. Singha, R., Rangarib, V., Sanagapallia, S., Jayaramana, V., Mahendraa, S., Singha, V. (2004). Nano-structured CdTe, CdS and TiO2 for thin film solar cell applications. *Solar Energy Materials& Solar Cells*, 82, 315-330.
2. Ali M. Mousa,A.J.Haider;Performance of a nanoCdS/Si Hetrojunction Deposited by CBD; Journal of Materials Science and Engineering A1 (**2011**) 111-115.
3. M. Bass, E.W. Van Stryland, D.R. Williams, W.L. Wolfe, Handbook of Optics, Vol. II, McGraw-Hill, USA, 1995, p. 36
4. H. Zogg, W. Vogt, H. Melchior, Nucl. Instrum.Methods Phys. Res., Sect. A, Accel.Spectrom. Detect. Assoc. Equip. 253 (1987) 418.
5. K.L. Chopra, R.C. Kainthla, D.K. Pandya, A.P. Thakoor, Phys. Thin Films12 (1982) 167.
6. R.S. Mane, C.D. Lokhande, Mater. Chem. Phys. 65 (2000) 1.
7. E.A. Streltsov, N.P. Osipovich, A.S. Lyakhov, L.S. Ivashkevich, Inorg. Mater.33 (1997) 442.
8. Alex P. Gaiduk , Peter I. Gaiduk, Arne Nylandsted Larsen ; Chemical bath deposition of PbSnanocrystals: Effect of substrate Thin Solid Films 516 (2008) 3791–3795.
9. Anna Osherov, Janos P Makai, Janos Balazs, ZsoltJHorvath, NadavGutman, Amir Sa'ar and Yuval Golan, Tunability of the optical band edge in thin PbS films chemically deposited on GaAs(100); J. Phys.: Condens. Matter 22 (2010) (1-6).
10. D. M. N. M. Dissanayake,a_ Ross A. Hatton, Thierry Lutz, Cristina E. Giusca, Richard J. Curry, and S. R. P. Silva,A PbS nanocrystal-C60 photovoltaic device for infrared light harvesting; APPLIED PHYSICS LETTERS **91**, 133506 (2007).
11. V. Stancu, E. Pentia, A. Goldenblum, M. Buda, G. Iordache, T. Botila, A Comparative Study of Microcrystalline and Nanocrystalline Lead Sulfide Based PbS/SiO2/Si Heterostructures; ROMANIAN JOURNAL OF INFORMATION SCIENCE AND TECHNOLOGY Volume 10, Number 1, 2007, 53-66.
12. Harumi Moreno-García, M.T.S. Nair, P.K. Nair, Chemically deposited lead sulfide and bismuth sulfide thin films and Bi2S3/PbS solar cells, Thin Solid Films 519 (2011) 2287–2295.
13. B. Sapoval and C. Hermann, "Physics of Semiconductors", Springer-Verlag, New York, 1995
14. R. A. Ismail, O.A. Abdulrazaq and J. Koshaba, "Materials Letters" , 60, 2006,2352.